MOLECULAR AND CELLULAR BIOLOGY, Sept. 1995, p. 5017–5029 Vol. 15, No. 9
0270-7306/95/$04.00+0

Characterization of a Novel 350-Kilodalton Nuclear Phosphoprotein That Is Specifically Involved in Mitotic-Phase Progression

XUELIANG ZHU,[1] MICHAEL A. MANCINI,[1] KAI-HSUAN CHANG,[1] CHIA-YANG LIU,[1] CHI-FEN CHEN,[1] BEI SHAN,[1] DIANE JONES,[1] TERESA L. YANG-FENG,[2] AND WEN-HWA LEE[1]*

Center for Molecular Medicine, Institute of Biotechnology, University of Texas Health Science Center at San Antonio, San Antonio, Texas,[1] and Department of Human Genetics, School of Medicine, Yale University, New Haven, Connecticut[2]

Received 26 April 1995/Returned for modification 30 May 1995/Accepted 13 June 1995

A gene assigned to human chromosome 1q32-41 encodes a novel protein of 3,113 amino acids containing an internal tandem repeat of 177 amino acids. The protein, which we have named "mitosin," was identified by direct binding to purified retinoblastoma protein in vitro with a region distantly related to the retinoblastoma protein-binding site of E2F-1. Mitosin is expressed throughout S, G_2, and M phases of the cell cycle but is absent in G_1. Its localization is dramatically reorganized from a rather homogeneous nuclear distribution in S phase to paired dots at the kinetochore/centromere region, to the spindle apparatus, and then to the midbody during M-phase progression. This spatial reorganization coincides closely with the temporal phosphorylation patterns of mitosin. Overexpression of N-terminally truncated mutants blocks cell cycle progression mainly at G_2/M. These results suggest that mitosin may play an important role in mitotic-phase progression.

Eukaryotes have evolved an elaborate mechanism to ensure accurate distribution of the genome to daughter cells. How chromosomes segregate properly during mitosis has been a fascinating question in modern biology. The centromere, located at the primary constriction of each chromosome, contains a complicated protein-DNA complex critical for chromosome segregation during mitosis. Electron microscopic studies have revealed a three-layer structure at the centromere: (i) an electron-dense inner plate that is embedded in the outer surface of the centromeric chromatin, (ii) an electron-lucent middle zone, and (iii) an electron-dense outer plate. This trilaminar structure, the kinetochore, is the functional unit of the centromere responsible for attachment to the microtubules that radiate out from the mitotic poles (reviewed in references 2, 3, 4, and 48). Interaction between kinetochores and microtubules is thought to be essential for chromosome segregation. Dysfunction of the kinetochore is therefore believed to be related to aneuploidy resulting from improper chromosome segregation.

Proteins residing at the mammalian centromere, known as the centromere proteins (CENPs in the nomenclature of Earnshaw and Rothfield [19]), have been identified through the study of autoantibody to centromere from patients with the CREST syndrome (calcinosis, Raynaud phenomenon, esophageal dysmotility, sclerodactyly, and telangiectasia) (43) and of antibodies prepared against purified chromosome scaffolds. Several CENPs have been characterized at the molecular level. CENP-A (17 kDa) is a centromere-specific core histone H3 variant and may have a direct role in centromeric chromatin packaging (45). CENP-B (80 kDa) binds to a 17-bp sequence within human α-satellite DNA (41). The localization of CENP-B beneath the kinetochore suggests that it may be involved in the formation of the centromeric heterochromatin (12). CENP-C (140 kDa) is a component of the inner kinetochore plate (49). Its absence in the inactive centromere of a stable dicentric chromosome therefore indicates that CENP-C may be required for kinetochore activity (16, 18). CENP-E (312 kDa) is a kinesin-like protein, and its transient association with the kinetochore during congression, followed by the relocation to the spindle midzone, reveals that it is likely to be a motor for chromosome movement and/or spindle elongation (38, 59, 60). In addition, the cytoplasmic dynein has also been found transiently attached to the kinetochore during M phase and may assist the process of chromosome segregation (56).

Genomic instability is a well-recognized hallmark of the neoplastic process and has consequently become a major focus of molecular cancer research. One tumor suppressor gene, p53, has been implicated in cancer-related genomic derangement via the loss of normal regulation of a checkpoint for the G_1/S transition (reviewed in reference 23). Aneuploidy, or alteration of chromosome numbers, is another common form of genomic instability and apparently results from improper chromosomal segregation in M phase. The strong association of aneuploidy with cancer suggests that altered regulation of the mitotic process could contribute substantially to oncogenesis. For example, alterations that remove mitotic checkpoints while preserving daughter cell viability could confer a clonal-growth advantage. This pathway for cancer formation is plausible but remains largely unexplored.

Associations of oncoproteins with proteins involved in chromosome segregation provide possible links between tumorigenesis and aneuploidy. By using transgenic mice expressing the large T antigen under specific control of the elastase 1 gene promoter, the sequential appearance of tetraploid and multiple aneuploid cell populations has been observed in pancreatic tissue (37). This study indicated that the expression of T antigen interferes with normal chromosomal segregation during M phase. It is also known that T antigen promotes entry into the cell cycle by removing growth inhibition factors. The retinoblastoma protein (Rb), which negatively regulates cell growth by controlling G_1 entry, is a cellular target of T antigen (reviewed in references 20 and 57). Rb is hypophosphorylated during early G_1 phase, hyperphosphorylated during late G_1 through G_2, and undergoes dephosphorylation during M (6, 8, 39). The hypophosphorylated form of Rb binds to both viral

* Corresponding author. Mailing address: Center for Molecular Medicine, Institute of Biotechnology, University of Texas Health Science Center at San Antonio, 15355 Lambda Dr., San Antonio, TX 78245. Phone: (210) 567-7353. Fax: (210) 567-7377.

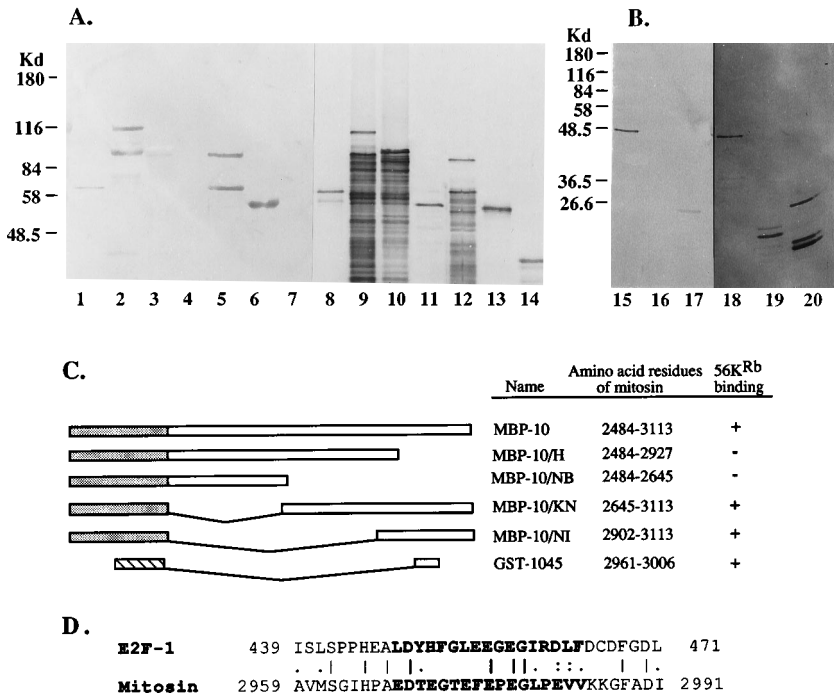

FIG. 1. Determination of the Rb-binding region of mitosin. (A) Two identical blots containing seven purified MBP fusion proteins were probed with either the Rb sandwich (52) (lanes 1 to 7) or an antibody against MBP (New England Biolabs) (lanes 8 to 14). Only those fusion proteins sharing the extreme C-terminal region of 211 amino acid residues of mitosin bound to the Rb sandwich. The faint band in lane 3 (MBP-10/H) is an artifact because it reproducibly migrated faster than the full-length product (lane 10). Lanes 1 and 8, MBP-T antigen as positive control; lanes 2 and 9, MBP-10; lanes 3 and 10, MBP-10/H; lanes 4 and 11, MBP-10/NB; lanes 5 and 12 were MBP-10/KN; lanes 6 and 13, MBP-10/NI; lanes 7 and 14, MBP alone. (B) Two identical blots of the purified GST fusion proteins were probed either with the Rb sandwich (lanes 15 to 17) or with an antibody to GST (30) (lanes 18 to 20). Lanes 15 and 18, GST-T antigen; lanes 16 and 19 GST alone; lanes 17 and 20, GST-1045, which bound to the Rb sandwich. The signal in lane 17 is positive, albeit weak. (C) Fusion proteins with their Rb-binding abilities. Open boxes, mitosin; shaded and hatched boxes, MBP and GST proteins, respectively. (D) Sequence comparison of the Rb-binding region (boldfaced) of mitosin and the neighboring residues with those of E2F-1. A 27% identity (48% similarity) between these two sequences was found. Vertical lines, identical residues; dots, conserved residues.

transforming proteins and all cellular Rb-associated proteins characterized thus far. Direct microinjection of unphosphorylated Rb inhibits G_1 progression (21). These results strongly suggest that the hypophosphorylated form of Rb is active in controlling G_1 entry. A recent article suggested that overexpression of Rb may arrest cells at G_2 (31). Although hypophosphorylated Rb does exist during mitotic phase, a role for Rb in M is not yet established. Two cellular proteins, phosphatase type 1a (15) and human nuc2 protein (9), have been shown to be associated with Rb during M phase. Interestingly, temperature-sensitive mutants of the yeast counterparts of these genes arrest yeast cells in M phase at the nonpermissive temperature (5, 14, 27). These data indirectly support a potential role for Rb in M-phase progression.

We describe here the characterization of a novel cell-cycle-dependent nuclear phosphoprotein, mitosin, which binds to Rb and probably plays an important role in mitotic-phase progression.

MATERIALS AND METHODS

Cloning and sequence analysis of mitosin cDNAs. Cloning of the cDNAs for Rb-associated proteins by the Rb sandwich method was described previously (52). Three additional libraries with cDNA fragments cloned via *Eco*RI were used for screening of full-length mitosin cDNA: Y79 cDNA library (35), K562 cDNA library, and H1262 cDNA library (the latter two were generous gifts from M.-L. Chu at Thomas Jefferson University, Philadelphia, Pa.). All cDNA inserts from isolated clones were obtained for further analysis either by subcloning into pGEM-3Z (Promega) or by conversion into the pBluescript plasmid from the Lambda Zap II vector (Stratagene). The orientation of the DNA inserts was determined by directly sequencing through intact *Eco*RI junctions. DNA sequencing was performed by the dideoxynucleotide termination method, and the sequences were analyzed with a computer program provided by DNASTAR (Madison, Wis.).

Plasmid construction. For the in vitro Rb-binding assay, different deletion mutants were derived from pMBP-10, which expresses a fusion of maltose-binding protein (MBP) and the C terminus of mitosin used to raise antimitosin antibody α10C (see below). The 3′-coding sequence of mitosin in pMBP-10 was deleted to either the *Hin*dIII site at nucleotide position 8849 or the *Nhe*I site at nucleotide position 8004 to express MBP-10/H (amino acid residues 2484 to 3027) and MBP-10/NB (residues 2484 to 2672). The 5′-coding sequence of mitosin cDNA in pMBP-10 was partially deleted to express MBP-10KN (residues 2645 to 3113) and MBP-10NI (residues 3002 to 3113), respectively. A *Bsp*HI-*Nco*I fragment (~0.14 kb) containing sequences homologous to the Rb-binding domain in E2F-1 was cloned into the unique *Nco*I site of pGEX-PK, a vector derived from pGEX-2T (7), to express GST-1045 (residues 2961 to 3006).

Three different expression plasmids were constructed to produce immunogens for antibodies against mitosin: (i) the insert from clone Ap10 was ligated in frame into pMAL-P (New England Biolabs) to express MBP fusion protein MBP-10, which contains amino acid residues 2484 to 3113 of mitosin, and (ii) the fragment encoding amino acid residues 1759 to 2093 and (iii) the fragment corresponding to residues 2092 to 2487 from clone Bla1 (see Fig. 7A) were cloned into pGEX-3X (Pharmacia) to express glutathione *S*-transferase (GST) fusion proteins (55) GST-10Bgl and GST-10Stu.

The vector pCEP4 (Invitrogen) was used to express mitosin in eukaryotic cells. This vector utilizes a cytomegalovirus promoter for high-level transcription, carries a hygromycin-resistant gene for selection, and replicates episomally. To distinguish the exogenously expressed mitosin from the endogenous form, a new plasmid, pCEP4F, containing the ATG sequence following the FLAG epitope was created by annealing oligonucleotide 5′CATGGACTACAAGGACGAC GATGACAAGA3′ and oligonucleotide 5′AGCTTCTTGTCATCGTCGTCCT TGTAGTCCATGGTAC3′ (28) and inserting the double-stranded oligonucleotide between the multiple cloning sites *Kpn*I and *Hin*dIII of pCEP4. To construct pCF-10, p10XL1 was digested with *Cla*I, filled in with Klenow enzyme, and then cut with *Not*I; the resulting 7.7-kb fragment was inserted into pCEP4F between the *Not*I and *Bam*HI sites (filled in with Klenow enzyme) to keep it in frame with the FLAG-coding sequence. pCF-10 was then cleaved with *Xho*I and *Not*I, filled in with Klenow, and then religated to create pCF-10Xh. pCF-10NN was constructed by cloning the *Nhe*I fragment of mitosin cDNA into the *Nhe*I site of

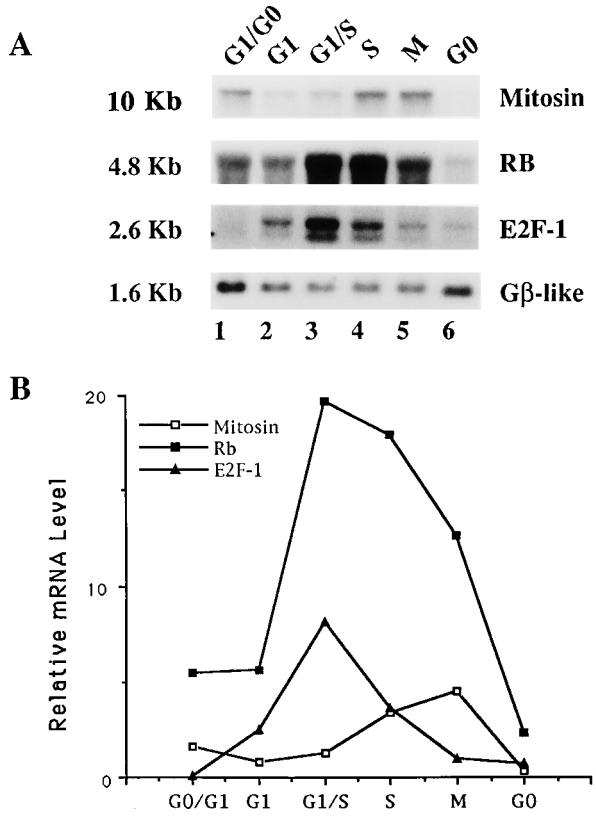

FIG. 2. Mitosin mRNA is expressed in a cell-cycle-dependent manner. (A) RNA blotting analysis using mitosin, RB, E2F-1, and Gβ-like cDNAs as probes. Monkey kidney CV1 cells were synchronized as described in Materials and Methods. Ten micrograms of total RNA extracted from each sample was subjected to Northern blotting with radioactively labeled cDNAs as indicated. The level of Gβ-like mRNA varies very little during the cell cycle and thus served as an internal control. Lane 1, RNA from cells arrested in early G_1 by lovastatin; lane 2, cells in late G_1 after removal of lovastatin for 8 h; lane 3, cells arrested at the G_1/S boundary by hydroxyurea; lane 4, cells in S phase, after removal of hydroxyurea for 5 h; lane 5, mitotic cells collected after a hydroxyurea-and-nocodazole double block; lane 6, G_0 cells after 4 days of serum starvation (0.5% fetal calf serum). (B) Quantitation of relative mRNA levels of each gene by densitometry. Each individual mRNA band was normalized to the amount of Gβ-like mRNA to show the expression pattern during the cell cycle.

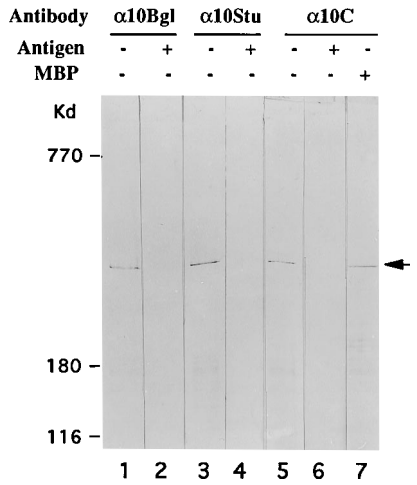

FIG. 3. Mitosin migrates as a 350-kDa cellular protein. About 10^6 actively growing HeLa cells were immunoprecipitated with each antibody against mitosin (α10Bgl, α10Stu, or α10C). After 3 to 12% gradient SDS-PAGE, the immunoprecipitates were immunoblotted with the same antibody in the absence (−) or presence (+) of the corresponding antigen competitor or MBP (10 μg/ml) to demonstrate specificity. A sample prepared from rabbit backbone muscles was also loaded side by side as a molecular weight marker; the position of nebulin (770 kDa) was visualized by immunoblotting with monoclonal antibody to nebulin (32a).

pCEP4F. All the constructs were confirmed by sequencing to ensure the correct reading frames.

Fusion protein expression and production of specific antibodies to mitosin. Expression of fusion proteins was induced by adding IPTG (isopropyl-β-D-thiogalactopyranoside) to a final concentration of 0.1 mM into an exponentially growing bacterial culture at 30°C. After 1 h of induction, bacteria were collected and lysed by mild sonication. Fusion proteins were purified either by electroelution after sodium dodecyl sulfate-polyacrylamide gel electrophoresis (SDS-PAGE) or by affinity chromatography.

Rabbits and mice were immunized subcutaneously with bacterially expressed fusion proteins GST-10Bgl (containing amino acids 1759 to 2093 of mitosin), GST-10Stu (2094 to 2487), and MBP-10 (2484 to 3113) by employing standard procedures. Immune sera (α10C, α10Bgl, and α10Stu) were purified by affinity chromatography using corresponding antigens.

Cell cycle synchronization. Normal monkey kidney CV1 cells were synchronized by different drugs to obtain uniform populations at different stages of the cell cycle. (i) For G_1 synchronization, cells grown in complete Dulbecco's modified Eagle medium plus 10% serum were supplemented with lovastatin (40 μM) for 36 h to be arrested at early G_1 (32). Cells were then released by adding mevalonic acid lactone to a final concentration of 4 mM for different periods. (ii) Synchronization at the G_1/S boundary was achieved by adding hydroxyurea (0.5 mM) (1) for 24 h; cells were then released from the arrest by three washes with phosphate-buffered saline (PBS) and incubation for different periods. (iii) For samples released from nocodazole block (prometaphase) (62), cells were initially synchronized by hydroxyurea. After three washes with PBS, medium with nocodazole (0.4 μg/ml) was added. Mitotic cells were collected by gently shaking off the dishes 12 h later. Following three more washes with PBS, aliquots of cells were replated for periods required by the experiments.

RNA blotting analysis. Total RNA was prepared from cells as described previously (51). Ten micrograms of each was denatured in 50% formaldehyde–20 mM sodium borate (pH 8.3), separated by 1% agarose gel electrophoresis, and then transferred to a Hybond membrane (Amersham) as suggested in the manufacturer's protocol. Northern (RNA) hybridization was performed as described elsewhere (51) with appropriate probes.

$^{32}P_i$ labeling and dephosphorylation by CIAP treatment. CV1 cells (2×10^6), released for 4 h from the hydroxyurea block at the G_1/S boundary, were labeled with $^{32}P_i$ (0.25 mCi/ml) (New England Nuclear) in phosphate-free Dulbecco's modified Eagle medium supplemented with 10% dialyzed fetal bovine serum for 2 h (54). Equal amounts of cells were collected by the mitotic shake-off after double blocking with hydroxyurea and nocodazole. These two different cell samples were lysed and immunoprecipitated with α10Bgl antibody. Immunoprecipitates from each sample were divided into two equal aliquots. Twenty units of calf intestinal alkaline phosphatase (CIAP; 20 U/ml; Boehringer Mannheim) in 25 μl of working buffer (50 mM Tris-HCl [pH 8.5], 0.1 mM EDTA) was added to one aliquot, while only 25 μl of buffer (without CIAP) was added to the remaining aliquot. Both fractions were incubated at 37°C for 10 min. Samples were then subjected to immunoblotting (52) or autoradiography.

Indirect immunofluorescence studies. Cells were washed in PBS and fixed for 20 min in cold methanol. After hydration in TBST (100 mM Tris-HCl [pH 7.4], 150 mM NaCl, 0.1% Tween 20), cells were blocked for 30 min in TBST containing 0.5% bovine serum albumin (TBST-BSA). A 1-h incubation with suitable antibody diluted in TBST-BSA was followed by another 1-h incubation with fluorochrome-conjugated secondary antibody (1:100) (Fisher Biotech). Nuclear DNA was then stained by DAPI (4′,6-diamidino-2-phenylindole) (0.5 μg/ml). Competition experiments were performed by including competitors (GST-10Bgl, GST-10Stu, MBP-10, or MBP; 10 μg/ml) to diluted antibodies. Chromosome spreads were prepared by centrifuging KCl-swollen mitotic CV1 cells onto coverslips (17) and then processed as described above, except that chromosomal DNA was stained by propidium iodide (1 μg/ml; Sigma) after RNase digestion. Samples were mounted in Permafluor (Lipshaw-Immunon, Inc.). Laser-scanning confocal microscopy was performed with a Zeiss LSM 310, equipped with Ar and HeNe lasers. Optical sections were digitized and superimposed with Normarski differential interference contrast images. The resulting images were directly recorded onto Ektachrome 100 film. Ektachrome P1600 was used when pictures were taken from a standard fluorescence microscope (Carl Zeiss, Inc.).

Chromosomal localization of the human mitosin gene. Two different approaches were performed to map the localization of the mitosin gene. First, a mapping panel (panel 1) of cell lines consisting of 17 mouse-human hybrids and 1 Chinese hamster-human hybrid was obtained from the National Institute of General Medical Sciences (NIGMS) cell repository. These hybrids and their human chromosome contents are described in detail in the NIGMS catalog. DNA samples were digested with *Pst*I, separated by gel electrophoresis, transferred to Hybond nylon filters (Amersham), and hybridized to the ^{32}P-labeled

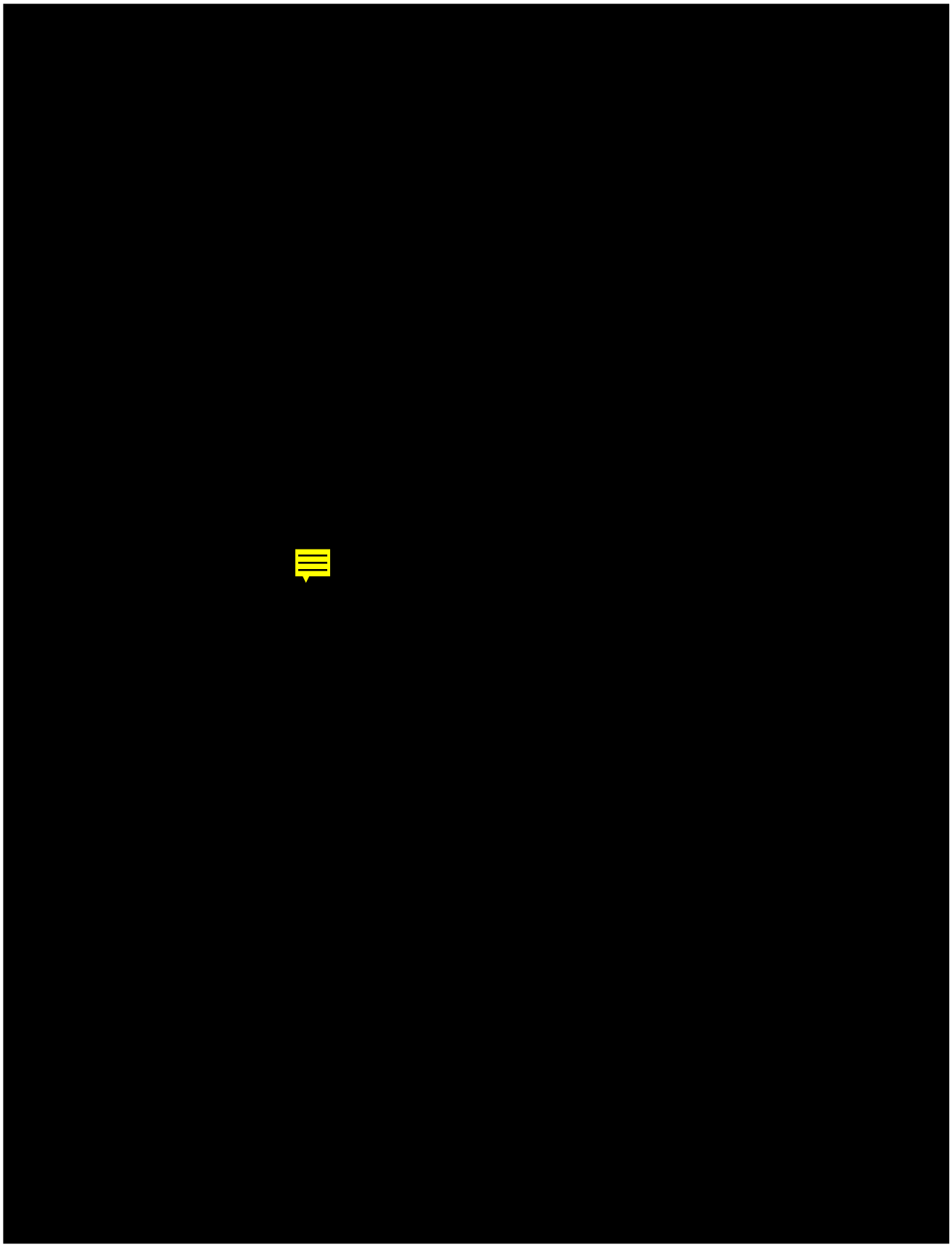

probe as described elsewhere (58). The second method was in situ hybridization. The Ap10 cDNA of mitosin was nick translated with [^{3}H]dATP and [^{3}H]dCTP to a specific activity of 3×10^7 cpm/μg and used for hybridization at a concentration of 25 ng/ml. Hybridization to normal human metaphase chromosomes, the posthybridization wash, emulsion autoradiography, and silver grain analysis were carried out as described previously (58).

Flow cytometry analysis. For determination of the extent of synchronization, CV1 cells arrested by different methods were trypsinized, washed once with PBS, and then fixed in 70% ethanol. After hydration in PBS, cells were stained overnight with 50 μg of propidium iodide per ml in the presence of RNase A (500 μg/ml). Fluorescence-activated cell sorting (FACS) analysis was performed with Coulter Epics Elite (Miami, Fla.).

For double-fluorescence analysis, 20 μg of each plasmid expressing FLAG-mitosin was transfected into CV1 cells by the calcium-phosphate method. After 3 days, cells were fixed with cold methanol. After hydration, the transfected cells were labeled with both anti-FLAG M2 antibody (Eastman Kodak) and fluorescein isothiocyanate-conjugated anti-mouse immunoglobulin G (Amersham) by a method similar to that for indirect immunofluorescence studies. After being washed with PBS, cells were resuspended into 2 ml of PBS, injected into 8 ml of cold methanol by using a 1-ml syringe with a 23-gauge needle, and fixed overnight. The fixed cells were then pelleted and labeled with propidium iodide. The cell cycle profiles of the fluorescein isothiocyanate-positive cells were then analyzed.

Nucleotide sequence accession number. The mitosin sequence has been deposited in GenBank (accession number U30872).

RESULTS

Interaction of mitosin with Rb in vitro. The function of Rb in cell growth and differentiation is believed to be exerted through association with other cellular proteins (20, 57). Consequently, we have used three different methods to identify cDNAs encoding proteins that bind to Rb, and 20 to 30 novel genes have been isolated (15, 47, 52). Mitosin cDNA was obtained by using the Rb sandwich method as described previously (52). To precisely define a region of mitosin responsible for binding to Rb, the original isolated clone AP10 containing a ~60-kDa portion of the C-terminal region of mitosin was fused to MBP and expressed in *Escherichia coli*. Four additional constructs containing deletion fragments of AP10 (Fig. 1C) and the first 300 amino acids of simian virus 40 large T antigen were fused to MBP and expressed. MBP alone served as a negative control. These seven MBP fusion proteins (Fig. 1, lanes 8 to 14) were blotted and probed with the Rb sandwich (52) (Fig. 1, lanes 1 to 7). Only the fusion proteins containing the C-terminal 211 amino acids of mitosin bound to Rb (Fig. 1, lanes 2, 5, and 6), with MBP-T antigen (lane 1) serving as a positive control. Interestingly, sequence comparison in Fig. 1D indicates that residues 2959 to 2991 of mitosin are distantly related to the region of the known Rb-binding domain in E2F-1 (25). To further demonstrate that this region of mitosin is sufficient to bind Rb, the mitosin fragment containing amino acid residues 2961 to 3006 was fused with GST to express fusion protein GST-1045. As shown in Fig. 1, both GST-T antigen (lane 15) and GST-1045 (lane 17) bound to Rb while GST alone (lane 16) did not. Thus, mitosin can specifically interact with Rb in vitro either by ligand screening an expression library or in a fusion protein-binding assay.

Expression of mitosin mRNA is cell cycle dependent. Because Rb function is modulated in concert with the cell division cycle, we first examined the expression pattern of this gene in synchronized primate cells. mRNA levels of mitosin in monkey kidney CV1 cells were low in G_1, gradually increased through S, and peaked in M phase (Fig. 2). This expression profile differed from those of three other genes: the transcription factor E2F-1, which is expressed predominantly at the G_1/S boundary; RB, which is expressed throughout the cell cycle with a three- to fourfold increase during S phase (51), and the Gβ-like gene (22), which is expressed uniformly throughout the cell cycle (52) and served as an internal control for RNA loading. These results suggested that the expression of mitosin mRNA is temporally regulated in S phase. Mitosin mRNA was also detected in all human tumor cell lines tested, including HeLa (cervical tumor), Molt4 (leukemia), and Saos2 (osteosarcoma) (data not shown), suggesting that mitosin is expressed in most of human cells.

Mitosin is a nuclear protein which associates with the mitotic apparatus during M phase. Three distinct polyclonal antibodies against three different regions of the deduced gene product were raised in mice or rabbits by using GST or MBP fusion proteins as antigens (see Materials and Methods). After purification by affinity chromatography, these antibodies—α10Bgl, α10Stu, and α10C—all recognized a cellular protein with a molecular mass of approximately 350 kDa in HeLa cells by immunoblotting (Fig. 3). Detection of this protein was specifically abolished by corresponding antigen competitors (Fig. 3). The same protein was also detected in other cell lines including monkey kidney CV1, human leukemia Molt4, and osteosarcoma Saos-2 (data not shown). By immunostaining (Fig. 4A, panel 1) and subcellular fractionation (data not shown), it was determined that this protein was located in the nucleus. The immunostaining pattern with α10C was specifically abolished by the corresponding antigen MBP-10 (Fig. 4A, panel 3) but not affected by the MBP competitor (Fig. 4A, panel 1). Similar competition results were obtained with other mitosin antibodies, suggesting that the staining patterns of these antibodies are specific to mitosin.

Interestingly, only 20 to 30% of unsynchronized populations were immunopositive (Fig. 4A, panel 1), regardless of the method of fixation (results not shown), suggesting that the synthesis of mitosin protein was also cell cycle dependent. When CV1 cells were synchronized at early G_1 by lovastatin treatment (32) and then released for 1 h, virtually all of the cells were negative for mitosin protein. When hydroxyurea-treated cells were released from arrest at the G_1/S boundary (1), more than 90% exhibited nuclear staining (data not shown). Cell nuclei were uniformly labeled except for nucleoli (Fig. 4B, panel 1), a pattern which remained unchanged through the rest of interphase. The localization of mitosin, however, changed dramatically during M phase. In late G_2 or early prophase, brightly staining foci began to appear (Fig. 4B, panel 2). Following chromosome condensation, more discrete pairs of fluorescence spots were observed (Fig. 4B, panel 3). During metaphase, bright and discrete paired dots were visible on the chromosomes at the midplate, in addition to some

FIG. 4. Mitosin is redistributed from the nucleus to the centromere, spindle, and midbody during M-phase progression. Monkey kidney CV1 cells were grown directly on glass coverslips. After methanol fixation and labeling with α10C and fluorescein isothiocyanate-conjugated anti-rabbit immunoglobulin G antibody, indirect immunofluorescence microscopy was performed with a laser-scanning confocal microscope. Digitized optical sections (red) and Normarski differential interference contrast (DIC) images (green) were superimposed or recorded separately. (A) Immunostaining of mitosin was not affected by MBP (10 μg/ml) (panel 1) but was abolished by the same amount of antigen MBP-10 (panel 3). Panels 2 and 4, corresponding DIC images. (B) A representative cell at different stages of the cell cycle. Panels 1 through 4, S or G_2 phase, late G_2/early prophase, prophase, and metaphase, respectively; panels 5 and 6, anaphase; panels 7 and 8, telophase. (C) Centromeric staining of mitosin. The centromeric staining was not affected by MBP (10 μg/ml) (panel 1) but was abolished by MBP-10 (panel 3). Panels 2 and 4, corresponding DIC images. Immunostaining of mitosin (panel 5) in mitotic cells spun onto coverslips was superimposed with the corresponding chromosome staining by propidium iodide (panel 6) and DIC image (panel 7) to confirm its centromeric localization (panel 8). Noncentromeric background labeling in panels 5 and 8 is due to the cytoplasmic portion of mitosin.

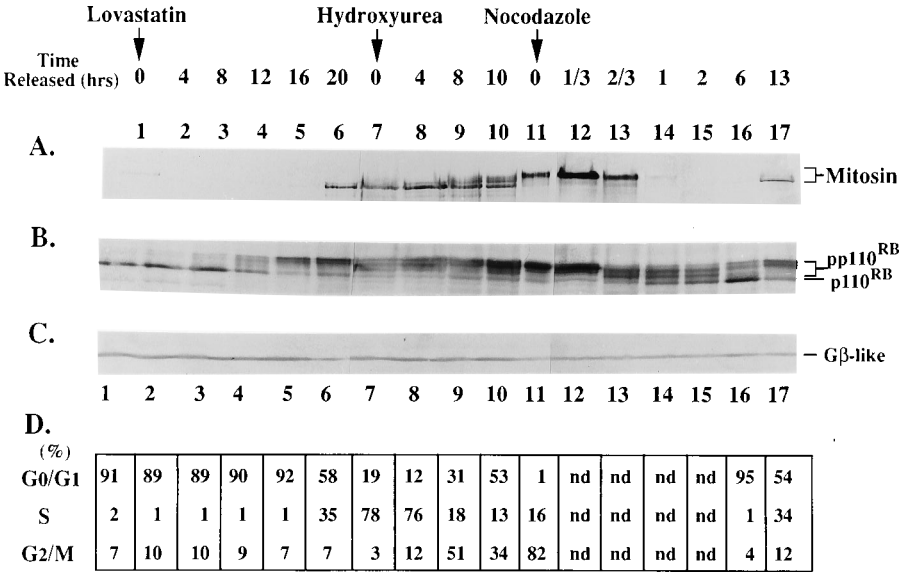

FIG. 5. Expression and modification of mitosin during the cell cycle. Cell lysates prepared from synchronized CV1 cells as described in Materials and Methods were analyzed by Western blotting. The appropriate portions of a blot (according to the molecular weights of proteins to be probed) were separately probed with antimitosin α10C (A), anti-Rb monoclonal antibody 11D7 (B), or anti-Gβ-like protein antibody (C). The phosphorylation status of Rb served as an internal control for the quality of synchronization. Gβ-like protein expressed constantly during the cell cycle was used as an internal control for quantitation of cell lysates. (D) Cell cycle distribution of the corresponding samples analyzed by flow cytometry to show the status of cell cycle progression. nd, not determined.

labeling in the spindle pole regions (Fig. 4B, panel 4). The intensity of the fluorescent dots decreased during anaphase; the staining at the spindle region became predominant (Fig. 4B, panels 5 and 6). During telophase, the midbody was labeled while the cytoplasmic staining decreased (Fig. 4B, panels 7 and 8). Following completion of cytokinesis, no immunostaining was observed (data not shown). The mitotic stages of these cells described above were determined by DAPI staining of nuclear DNA (data not shown).

To substantiate that mitosin is located at the centromere, chromosome spreads prepared from nocodazole-arrested CV1 cells were used for immunostaining. As shown in Fig. 4C, panels 5 through 8), mitosin was unambiguously found at the centromere region. The specificity of the centromeric staining was further confirmed by competition experiments (Fig. 4C, panels 1 through 4). Identical staining patterns were obtained with either α10Bgl or α10Stu. These results confirmed that mitosin transiently associated with the centromere in M phase. Colocalization results with CREST antisera by immunogold electron microscopy indicate that mitosin directly associates with the outer kinetochore plate (61).

Mitosin is synthesized and phosphorylated in a cell-cycle-dependent manner. To corroborate the immunostaining observations, we analyzed synchronized cell populations by Western blotting (immunoblotting). Using lovastatin (33), hydroxyurea (1), and nocodazole (62), CV1 cells were synchronized at various stages of the cell cycle. The degree of synchronization was confirmed by the expression pattern of Rb (Fig. 5B) (6, 8) as well as by flow cytometry (Fig. 5D). Mitosin was virtually undetectable in G1 (lanes 1 to 5 and 14 to 16), appeared when cells entered S phase, peaked in M phase (lanes 6 to 13), and then rapidly disappeared (lanes 14 and 15), as shown in Fig. 5A. Immunofluorescence studies with the same set of samples exhibited the same expression pattern of mitosin (data not shown). In contrast, the level of Gβ-like protein remained unchanged throughout the cell cycle (Fig. 5C). In addition to the difference in protein quantity, the mobility of mitosin in SDS-PAGE gradually decreased, suggesting the possibility of posttranslational modification. The appearance of the multiple, slowly migrating mitosin isoforms suggested a stepwise modification between late S phase and prophase of mitosis. After prometaphase (the block point of nocodazole), only the most slowly migrating form was present, and it disappeared rapidly thereafter.

To test whether mitosin was modified by phosphorylation, CV1 cells synchronized in mid-S phase were labeled in the presence of $^{32}P_i$ and the cell lysates were immunoprecipitated by α10Bgl. As shown in Fig. 6B, mitosin was radiolabeled with ^{32}P, and the label was removed when immunoprecipitates were treated with CIAP. The same gel was also immunoblotted with mitosin antibody to confirm the existence of mitosin after CIAP treatment (Fig. 6A). A similar experiment was performed with cells synchronized in M phase, in which the most slowly migrating form of mitosin was converted into the fastest-migrating form by CIAP (Fig. 6C). These results clearly

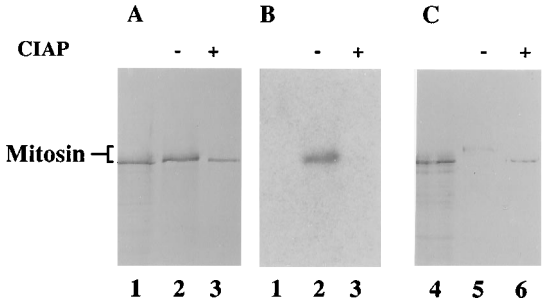

FIG. 6. Modification of mitosin by phosphorylation. (A and B) Immunoblotting and autoradiography of the same blot, respectively. Lanes 1 and 4, mitosin prepared from cells arrested at G_1/S by hydroxyurea; lanes 2, mitosin immunoprecipitated from cells in mid-S phase, labeled with $^{32}P_i$; lanes 3, same sample treated with CIAP. (C) The most slowly migrating, M-phase form of mitosin (lane 5) was converted to the fastest-migrating form by CIAP treatment (lane 6).

TABLE 1. Correlation of the presence of the human mitosin gene with the presence of human chromosomes in human-rodent somatic-cell hybrids

Chromosome	No. of hybrids[a]					Total[b]	% Discordant
	Concordant		Discordant				
	+/+	−/−	+/−	−/+	Total		
1	4	14	0	0	0	18	0
2	3	11	1	3	4	18	22
3	3	7	1	6	7	17	41
4	4	7	0	5	5	16	31
5	2	7	1	7	8	17	47
6	4	6	0	8	8	18	44
7	4	6	0	6	6	16	38
8	4	5	0	6	6	15	40
9	0	13	4	1	5	18	28
10	2	8	1	2	3	13	23
11	0	8	3	4	7	15	47
12	2	6	1	8	9	17	53
13	3	10	0	2	2	15	13
14	4	5	0	8	8	17	44
15	4	6	0	5	5	15	33
16	1	13	2	1	3	17	18
17	4	3	0	11	11	18	61
18	4	10	0	4	4	18	22
19	4	9	0	2	2	15	13
20	4	7	0	6	6	17	35
21	1	7	2	7	9	17	53
22	2	8	1	5	6	16	38
X	0	11	3	1	4	15	27
Y	1	10	3	2	5	16	31

[a] + and −, presence and absence, respectively, of the gene sequence (first symbol) or the chromosome (second symbol).
[b] Chromosomes present at a frequency of 0.1 or less were excluded from the analysis.

demonstrate that phosphorylation is a major posttranslational modification and that the mobility shift is caused by hyperphosphorylation of mitosin. The temporal pattern of mitosin phosphorylation coincides closely with its spatial reorganization as shown in Fig. 4, suggesting that phosphorylation may be critical for these changes.

Primary structure of mitosin. To further characterize mitosin, we have completely sequenced the full-length cDNA and its primary amino acid sequence was deduced. Four of the cDNA clones originally isolated by the Rb sandwich screening (52) had identical 3′ sequences of ~2 kb. A series of overlapping clones spanning 10,211 bp was isolated by multiple screens of several different cDNA libraries (Fig. 7A). The longest open reading frame deduced from the DNA sequence encodes a protein of 3,113 amino acid residues. Its isoelectric point (pI) was predicted to be 5.1. The existence of multiple stop codons in all three reading frames upstream of the first ATG strongly suggested that the cDNA sequence defined by these clones was a full-length one (Fig. 7B).

The deduced amino acid sequence of mitosin is novel. It does not have significant homology with any known proteins in GenBank. Interestingly, this protein contains a pair of highly charged tandem repeats separated by two proline residues (Fig. 7C). The first repeat (residues 2110 to 2289) is 60% identical to the second (residues 2292 to 2471). This internal repeat region is flanked by two blocks of leucine heptad repeats (33). Additionally, seven leucine repeats are found near the N-terminal region, and another two are found close to the C-terminal region. The secondary structure of this protein is predicted to be mostly α-helical, except for the extreme C-terminal region of 220 residues, which is proline rich, has a pI of 10.2, and contains a putative bipartite nuclear targeting signal (13) and the Rb-binding region, as shown in Fig. 1.

Assignment of the mitosin gene to human chromosome 1q32-41. Determination of the localization of this gene in a human chromosome may provide additional information on its potential relationship with certain genetic diseases. We have performed Southern analysis with a panel of well-characterized mouse-human and Chinese hamster-human somatic cell hybrids to map the mitosin gene to human chromosome 1. The mitosin cDNA probe recognized a 3.5- and a 1.6-kb *Pst*I fragments in human genomic DNA, a 1.9-kb *Pst*I fragment in mouse DNA, and a 6.8-kb doublet in Chinese hamster DNA (data not shown). Both human-specific fragments were present only in hybrids containing human chromosome 1 (Table 1).

In situ hybridization of the cDNA probe to normal human metaphase spreads resulted in specific labeling at region q32-41 of chromosome 1 (Fig. 8). Thirty-two of 50 metaphase cells (60%) had silver grains over this specific region. Of 77 grains analyzed, 33 (42.9%) were located at 1q32-q41. No other site was labeled above background. Interestingly, alterations in this region have been found to be associated with several types of cancer including breast and lung cancers (36, 42).

Exogenous expression of truncated mitosins interrupts cell cycle progression. The cell-cycle-dependent expression of mitosin, its association with the kinetochore/centromere, and the chromosomal localization of the gene suggest a potential role of mitosin in cell cycle progression. To further substantiate this notion, we exogenously expressed several truncated mutants of mitosin tagged with the FLAG epitope (28) at their N termini (Fig. 9A) in CV1 cells. Expression of the epitope-tagged proteins was confirmed by Western blot (not shown) and by using indirect immunofluorescence microscopy by simultaneous staining of both the N-terminal FLAG epitope and the C-terminal region of mitosin with specific antibodies (Fig. 9B). Both pCF-10 and pCF-10Xh constructs produced fusion proteins localized primarily to the nucleus, while the fusion protein containing only the tandem repeat (pCF-10NN) was found localized only in the cytoplasm. Transfection with the vector alone (pCEP4F) did not express any detectable FLAG epitope (data not shown). The specificities of the antibodies used were further confirmed by the findings that anti-FLAG M2 does not cross-react with the endogenous mitosin which was recognized by mitosin α10C in untransfected cells (Fig. 9B) and the α10C antibodies do not recognize a FLAG fusion protein of a C-terminally truncated mitosin which has epitopes for α10C deleted (data not shown).

Severe inhibition of cell proliferation was observed in CV1 cells overexpressing pCF-10 and pCF-10Xh but not the mutant (pCF-10NN) or the vector alone. After transient transfection for 3 days, the transfected culture cells were stained with anti-FLAG M2 antibody. Virtually all cells expressing pCF-10 or pCF-10Xh appeared in isolation, whereas the majority of cells expressing pCF-10NN appeared in clusters of two to eight cells (data not shown). The transfected cells were further selected by hygromycin for 14 days. The majority of the pCF-10- or pCF-10Xh-transfected, hygromycin-resistant colonies were FLAG negative; some colonies contained only 1% FLAG-positive cells (Table 2), suggesting that the actively dividing cells were those which lost the expression of mitosin. Colonies transfected with the vector alone (pCEP4F) grew to a large size and contained no FLAG-positive cells. In contrast, 96% of colonies transfected with pCF-10NN were FLAG positive; and more than 60% of cells in a given colony were stained brightly by both anti-FLAG and α10C antibodies (Table 2), although

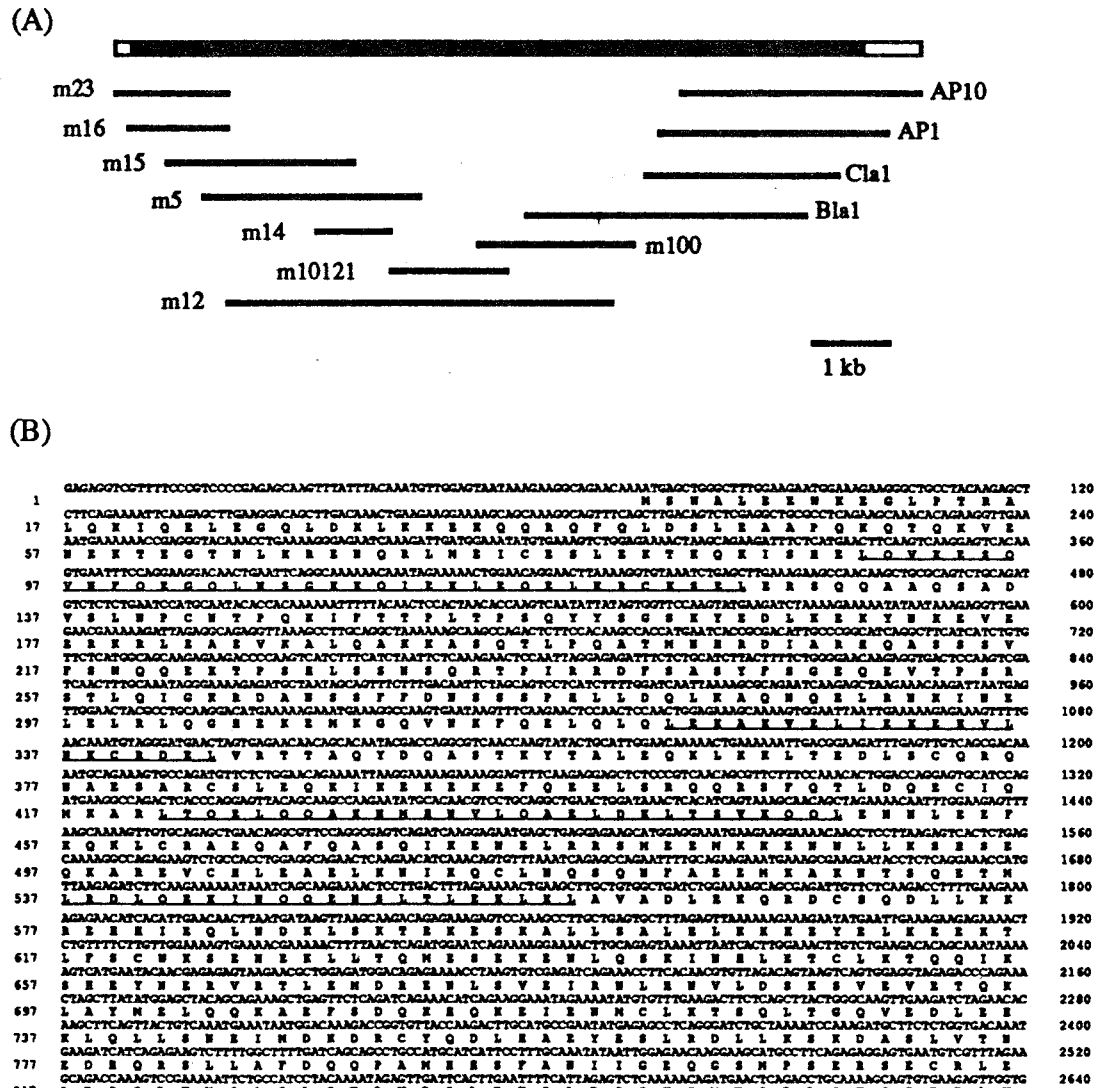

FIG. 7. Cloning and sequence analysis of mitosin. (A) Overlapping cDNA clones and the full-length cDNA. Open boxes, untranslated regions. The open reading frame is shaded. Clones AP10 and AP1 were isolated by the Rb-sandwich method. Clones C1a1, B1a1, and m100 were isolated from the Y79 cDNA library, clones m14 and m10121 were obtained from the K562 cDNA library, and the rest were from the H1262 cDNA library. (B) Nucleotide sequence and deduced amino acid sequence of mitosin. The putative leucine heptad repeats are underlined. (C) Alignment for the internal repeats. The sequences were found to have 60% identity and 75% similarity. Identical and similar residues are indicated (vertical lines and dots, respectively).

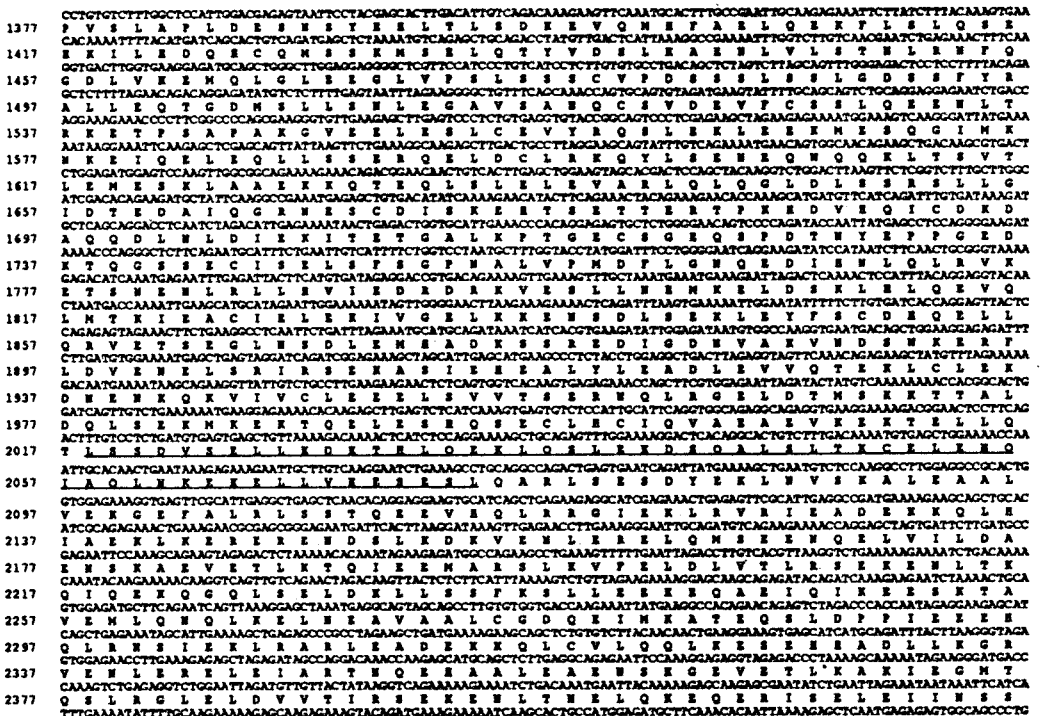

(C)

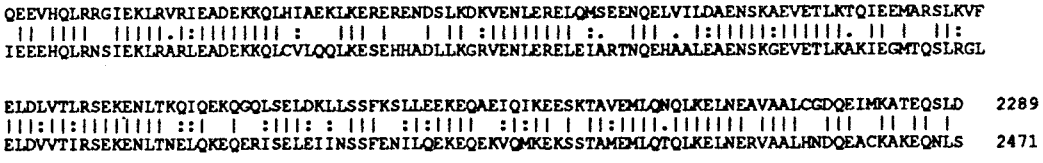

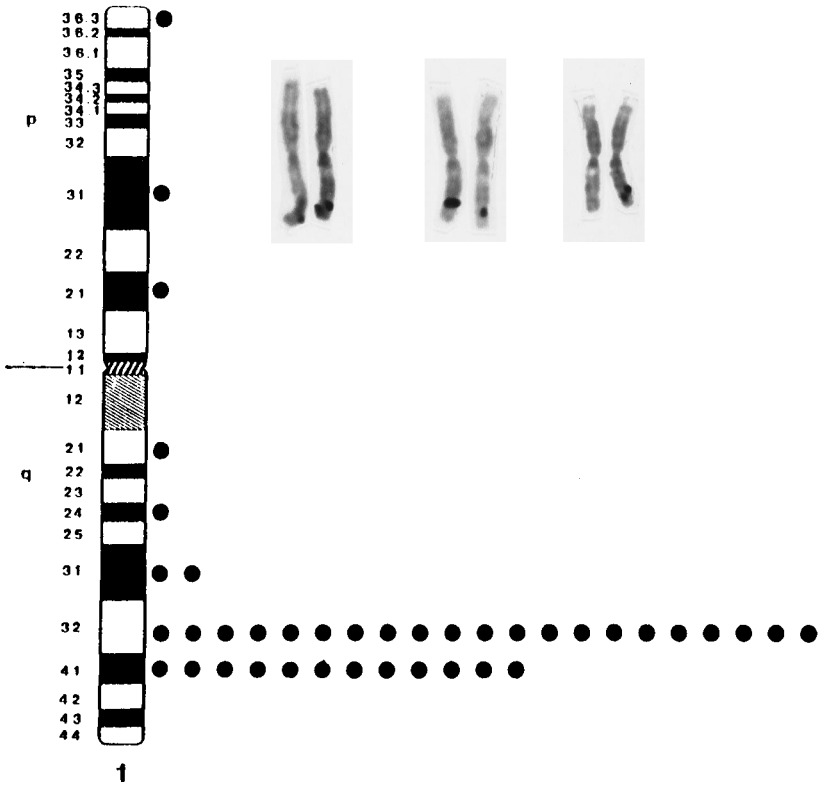

FIG. 8. Assignment of the mitosin gene to human chromosome 1q32-41. The cDNA probe of mitosin was nick translated with [^{3}H]dATP and [^{3}H]dCTP and used for hybridization to normal human metaphase chromosomes. Results of autoradiography and silver grain analysis of the chromosome 1 are shown.

the average colony size was smaller than those of the other three. The slower growth rate of these cells may be due to an overexpression of the exogenous protein which is frequently observed in tissue culture cells. Nevertheless, these results strongly suggest that overexpression of the N-terminally truncated mutant of mitosin severely inhibits cell growth.

To explore which cell cycle stage(s) of these transfected cells was accumulated, DNA contents of the cells expressing FLAG-tagged mitosin detected by anti-FLAG antibody were analyzed by staining with propidium iodide using FACS assay 3 days after transfection. Cells expressing pCF-10Xh showed a cell cycle distribution of (51 ± 4)% in G_0/G_1, (14.5 ± 0.5)% in S, and (34.5 ± 4.5)% in G_2/M. Cells expressing the C-terminally truncated mitosin (pCF-10NN) had an average of (62.5 ± 2.5)% in G_0/G_1, (17 ± 2)% in S, and (20.5 ± 4.5)% in G_2/M. These results were reproducibly derived from several separate experiments. The significant accumulation of the G_2/M population in cells overexpressing the N-terminally truncated mitosin suggests that the cells were retarded at G_2/M. Transfection of the CV-1 cells with pCF-10 frequently resulted in an extremely low expression efficiency [(0.03 ± 0.01)% of FLAG-positive cells], which hampered accurate analysis of cell cycle distribution.

DISCUSSION

Several lines of evidence described here suggest that mitosin may play a crucial role in mitotic-phase progression. First, mitosin is expressed only during S and G_2/M phases; it rapidly disappears upon the completion of mitosis. Second, mitosin is subjected to specific phosphorylation possibly during G_2/M transition. Third, during mitosis, mitosin undergoes a dynamic spatial reorganization to several components of the mitotic apparatus, e.g., the centromere and the spindle region, and this redistribution coincides closely with change in its phosphorylation state. Moreover, overexpression of the N-terminally truncated mutants led to accumulation of cells mainly at G_2/M.

The inhibition of G_2/M-phase progression by overexpression of N-terminally truncated mutant mitosins is particularly interesting. Recently, we found that the C-terminal region of mitosin contained a crucial domain for both dimerization with itself and heterodimerization with other cellular proteins (61). Therefore, the N-terminally truncated mutants may interact with themselves or other cellular proteins but interfere with normal function. This phenomenon is consistent with the previously proposed dominant-negative-mutation hypothesis (26).

The kinetochore/centromere and the spindle localization of mitosin suggest that it may function during chromosome segregation. The long leucine repeats in mitosin potentially form coiled-coil structures and may provide the means to allow interaction with other kinetochore proteins. It is known that hydrophobic heptad repeats may mediate protein-protein interactions through coiled-coil formation (11, 33). Several proteins have been identified to be components of the kinetochore/centromere (reviewed in reference 4). One, CENP-E (59, 60), has a predicted coiled-coil structure and behaves similarly to mitosin during mitosis. CENP-E is a kinesin motor believed to play important roles in chromosome movement and/or spindle elongation. During M phase, both CENP-E and mitosin are redistributed to the kinetochore, spindle, and midbody at the same stages of the cell cycle. However, unlike mitosin, CENP-E is synthesized shortly before mitosis and remains in the cytoplasm until prometaphase. Mitosin may therefore serve as a potential target for CENP-E redistribution

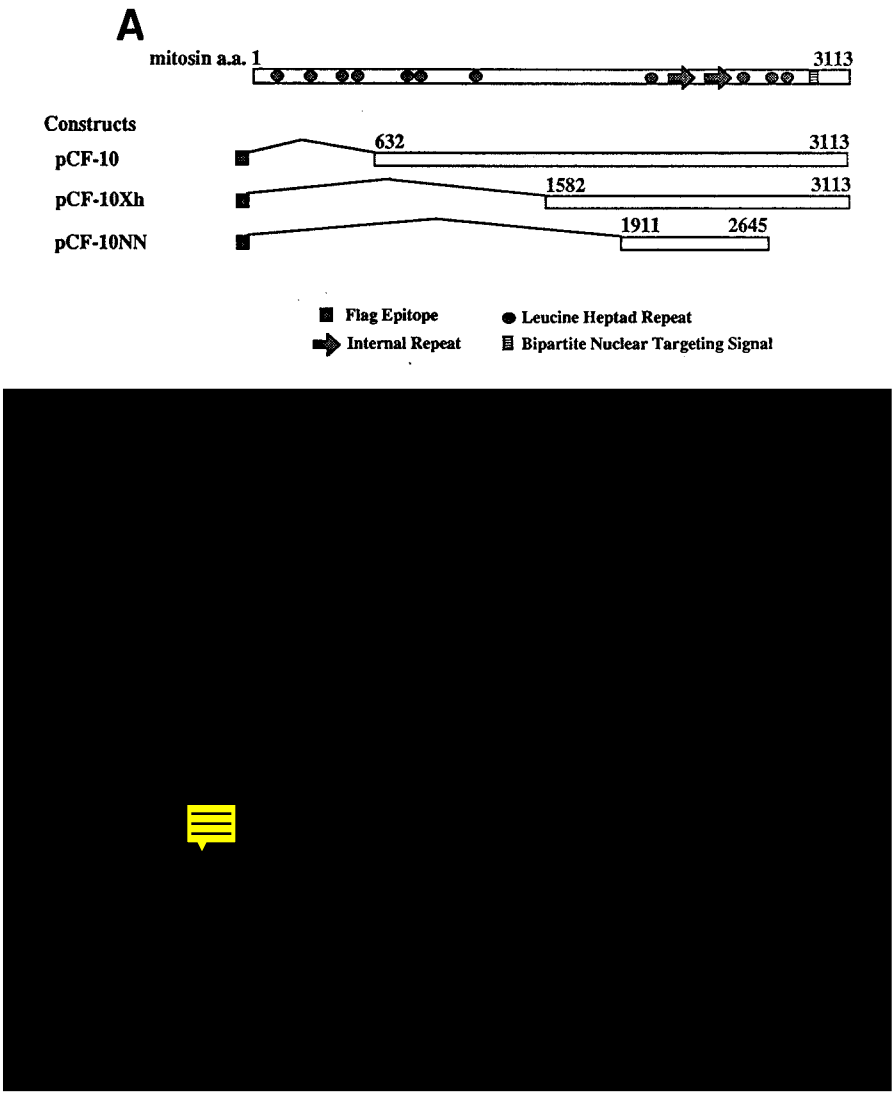

FIG. 9. Transient expression of mitosin in CV1 cells. (A) Mitosin expression constructs. a.a., amino acid. (B) Cells growing in 100-mm dishes were methanol fixed 48 h after transfection with mitosin-expressing plasmids and subjected to triple fluorescence staining. The extreme C terminus of mitosin stained green with α10C antibody and fluorescein isothiocyanate-conjugated anti-rabbit immunoglobulin G (panels 1, 4, and 7); the FLAG epitope stained red with anti-FLAG M2 and Texas Red-conjugated anti-mouse immunoglobulin G (panels 2, 5, and 8); nuclear DNA stained blue with DNA-specific dye DAPI (panels 3, 6, and 9). Panels 1 to 3, 4 to 6, and 7 to 9, transfections with pCF-10, pCF-10Xh, and pCF-10NN, respectively.

to the kinetochore. This hypothesis is testable since both genes have been cloned.

Modification of mitosin by phosphorylation may also be very critical to its proposed function in M-phase progression. The appearance of brightly staining foci of mitosin in nuclei is always accompanied by various degrees of chromatin condensation (data not shown), which is a hallmark of the initiation of prophase. As changes in the phosphorylation pattern occur in temporal correspondence with the reorganization of mitosin, and its subsequent degradation, the secondary modification of this protein may have a critical role for its function. It will be interesting to explore which kinase(s) regulates the phosphorylation of mitosin. Among these kinases, cdc2, which has been shown to be critical for the entry into M phase (for a review, see reference 44), may be the best candidate. There are five consensus sites for cdc2 kinase ($S/TPX_{0,1}R/K$) (53) located at positions 820 to 822 (SPK), 1684 to 1686 (TPK), 3011 to 3013 (SPR), 3082 to 3084 (SPR), and 3097 to 3099 (SPK) in mitosin; however, it remains to be shown whether these sites are the primary phosphorylation sites.

The potential role of mitosin in human disease is implicated by its chromosomal localization at 1q32-41. Abnormalities in human chromosome 1q have been reported to be involved in

TABLE 2. Effect of ectopic expression of mitosin on cell division

Construct	% Colonies with TR^{+a} cells	% TR^{+} cells/colony[b]	Approx no. of cells/colony[c]
pCF-10	20	1	100
pCF-10Xh	31	1	100
pCF-10NN	96	60	55
pCEP4F	0	0	100

[a] TR^{+}, Texas Red positive.
[b] For colonies with TR^{+} cells.
[c] Approximately 300 colonies were analyzed for each sample.

several types of cancer formation, e.g., breast cancer (for a review, see reference 36), lung cancer (reviewed in reference 42), and acute monocytic leukemia (24). Genes responsible for two other genetic disorders, Usher syndrome type II and Van der Woude syndrome, have been localized to the same region, 1q32-41, as mitosin (46, 50). Mitosin may serve as a candidate gene for these diseases, or as a marker for further linkage analysis.

We have, thus far, provided reasonable evidence suggesting that mitosin is important for mitotic-phase progression. However, the biological significance of the interaction between Rb and mitosin remains unclear. Since the mitosin gene was independently isolated four times by directly screening a λgt11 expression library with purified p56-Rb protein as probe, the interaction between these two proteins may not be fortuitous. With an in vitro binding assay, a specific region of mitosin (corresponding to amino acid residues 2959 to 2991) was found to bind Rb protein, again suggesting that the binding of mitosin to Rb is specific. However, an attempt to demonstrate such interaction in vivo has not been fully satisfactory. An interaction was found by an M-phase-specific coimmunoprecipitation of mitosin with antibody against Rb, but the reversal experiment using antimitosin antibodies has not been successful (data not shown). The latter case is probably due to the failure of antimitosin antibodies to recognize the Rb-mitosin complex in which the epitopes of mitosin are masked. Recently, we have also found that both mitosin and hypophosphorylated Rb can be detected in the chromosome scaffold (40).

What might the biological consequence of an Rb-mitosin interaction be? Cells without Rb such as retinoblastoma cells (35) and Rb-deficient mouse fibroblasts (10, 29, 34) successfully proceed through the cell cycle, suggesting that the interaction is not required for M-phase progression. If there is a function for such an interaction, it must be very subtle, for example, in proofreading the progression of chromosome segregation. Loss of such an association may consequently cause aneuploidy. This prediction is consistent with the previous observation that expression of the simian virus 40 T antigen in transgenic mice led to tetraploidy and then to aneuploidy in cells (37). Interestingly, two other important proteins involved in M-phase progression, phosphatase 1α and H-nuc, were associated with hypophosphorylated Rb (9, 15). The findings that Rb associates with important proteins functioning in mitotic phase will allow us to further investigate its role during mitosis and tumorigenesis.

ACKNOWLEDGMENTS

We thank K. Wang for the nebulin sample and antinebulin antibody, M.-L. Chu for cDNA libraries, P.-L. Chen for newly engineered vectors used in this study, and Tim Yen for the exchange of information which led to the mutual realization that mitosin and CENP-F are very similar.

This study was supported by grants from the National Institutes of Health (EY05758 and CA58318), the Texas Coordinated Board (ATP 003659-055), and the Council for Tobacco Research.

REFERENCES

1. **Adams, R. L., and J. G. Lindsay.** 1967. Hydroxyurea reversal of inhibition and use as a cell-synchronizing agent. J. Biol. Chem. **242:**1314–1317.
2. **Ault, J. G., and C. L. Reider.** 1992. Chromosome mal-orientation and reorientation during mitosis. Cell Motil. Cytoskel. **22:**155–159.
3. **Ault, J. G., and C. L. Rieder.** 1994. Centrosome and kinetochore movement during mitosis. Curr. Opin. Cell Biol. **6:**41–49.
4. **Bloom, K.** 1993. The centromere frontier: kinetochore components, microtubule-based motility, and the CEN-value paradox. Cell **73:**621–624.
5. **Booher, R., and D. Beach.** 1989. Involvement of a type 1 protein phosphatase encoded by bws1+ in fission yeast mitotic control. Cell **57:**1009–1016.
6. **Buchkovich, K., L. A. Duffy, and E. Harlow.** 1989. The retinoblastoma protein is phosphorylated during specific phases of the cell cycle. Cell **58:**1097–1105.
7. **Chen, P. L., and W.-H. Lee.** Unpublished data.
8. **Chen, P.-L., P. Scully, J.-Y. Shew, J. Y.-J. Wang, and W.-H. Lee.** 1989. Phosphorylation of the retinoblastoma gene product is modulated during the cell cycle and cellular differentiation. Cell **58:**1193–1198.
9. **Chen, P.-L., Y.-C. Ueng, T. Durfee, K.-C. Chen, T. Yang-Feng, and W.-H. Lee.** 1995. Identification of human homologue of yeast nuc2 which interacts with retinoblastoma protein in a specific manner. Cell Growth Differ. **6:**199–210.
10. **Clarke, A. R., E. R. Maandag, M. van Roon, N. M. T. van der Lugt, M. van der Valk, M. L. Hooper, A. Berns, and H. te Riele.** 1992. Requirement for a functional Rb-1 gene in murine development. Nature (London) **359:**328–330.
11. **Cohen, C., and D. A. D. Parry.** 1986. Alpha-helical coiled coils—a widespread motif in proteins. Trends Biochem. Sci. **11:**245–248.
12. **Cooke, C. A., R. L. Bernat, and W. C. Earnshaw.** 1990. CENP-B: a major human centromere protein located beneath the kinetochore. J. Cell Biol. **110:**1475–1488.
13. **Dingwall, C., and R. A. Laskey.** 1991. Nuclear targeting sequences—a consensus? Trends Biochem. Sci. **16:**478–481.
14. **Doonan, H. J., and N. R. Morris.** 1989. The bimG gene of Aspergillus nidulans, which is required for completion of anaphase, encodes a homolog of mammalian phosphoprotein phosphatase 1. Cell **57:**987–996.
15. **Durfee, T., K. Becherer, P.-L. Chen, S.-H. Yeh, Y. Yang, A. E. Kilburn, W.-H. Lee, and S. J. Elledge.** 1993. The retinoblastoma protein associates with the type 1 protein phosphatase catalytic subunit. Genes Dev. **7:**555–569.
16. **Earnshaw, W. C., R. L. Bernat, C. Cooke, and N. F. Rothfield.** 1991. Role of the centromere/kinetochore in cell cycle control. Cold Spring Harbor Symp. Quant. Biol. **LVI:**675–685.
17. **Earnshaw, W. C., N. Halligan, C. A. Cooke, and N. Rothfield.** 1984. The kinetochore is part of metaphase chromosome scaffold. J. Cell Biol. **98:**352–357.
18. **Earnshaw, W. C., H. Ratrie, and G. Stetten.** 1989. Visualization of centromere proteins CENP-B and CENP-C on a stable dicentric chromosome in cytological spreads. Chromosoma **98:**1–12.
19. **Earnshaw, W. C., and N. Rothfield.** 1985. The identification of a family of human centromere proteins using autoimmune sera from patients with scleroderma. Chromosoma **91:**313–321.
20. **Goodrich, D., and W.-H. Lee.** 1993. Molecular characterization of the retinoblastoma susceptibility gene. Biochim. Biophys. Acta **1155:**43–61.
21. **Goodrich, D. W., N. P. Wang, Y.-W. Qian, E. Y.-H. P. Lee, and W.-H. Lee.** 1991. The retinoblastoma gene product regulates progression through the G1 phase of the cell cycle. Cell **67:**293–302.
22. **Gullemont, F., A. Billault, and C. Auffray.** 1989. Physical linkage of guanine nucleotide-binding protein-related gene to the chicken major histocompatibility complex. Proc. Natl. Acad. Sci. USA **86:**4594–4598.
23. **Hartwell, L.** 1992. Defects in a cell cycle checkpoint may be responsible for the genomic instability of cancer cells. Cell **71:**543–546.
24. **Hawkins, J. M., M. Wood, F. Wright, and L. M. Secker-Walker.** 1992. Isochromosome 1q in acute monocytic leukemia: a new nonrandom association. Genes Chromosomes Cancer. **5:**181–183.
25. **Helin, K., J. A. Lees, M. Vidal, N. Dyson, E. Harlow, and A. Fattaey.** 1992. A cDNA encoding a pRB-binding protein with properties of the transcription factor E2F. Cell **70:**337–350.
26. **Herskowitz, I.** 1987. Functional inactivation of genes by dominant negative mutations. Nature (London) **329:**219–222.
27. **Hirano, T., Y. Hiraoka, and M. Yanagida.** 1988. A temperature-sensitive mutation of the Schizosaccharomyces pombe gene nuc2+ that encodes a nuclear scaffold-like protein blocks spindle elongation in mitotic anaphase. J. Cell Biol. **106:**1171–1183.
28. **Hopp, T. P., K. S. Prickett, V. Price, R. T. Libby, C. J. March, P. Cerretti, D. L. Urdal, and P. J. Conlon.** 1988. A short polypeptide marker sequence useful for recombinant protein identification and purification. Bio/Technology **6:**1205–1210.
29. **Jacks, T., A. Fazeli, E. M. Schmitt, R. T. Bronson, M. A. Goodell, and R. A. Weinberg.** 1992. Effects of an Rb mutation in the mouse. Nature (London) **359:**295–300.
30. **Jones, D., and W.-H. Lee.** Unpublished data.
31. **Karantza, V., A. Maroo, D. Fay, and J. M. Sedivy.** 1993. Overproduction of Rb protein after the G_1/S boundary causes G_2 arrest. Mol. Cell. Biol. **13:**6640–6652.
32. **Keyomarsi, K., L. Sandoval, V. Band, and A. B. Pardee.** 1991. Synchronization of tumor and normal cells from G1 to multiple cell cycles by lovastatin. Cancer Res. **51:**3602–3609.

32a. **Kruger, M., J. Wright, and K. Wang.** 1991. Nebulin as a length regulator of thin filaments of vertebrate skeletal muscles: correlation of thin filament length, nebulin size, and epitope profile. J. Cell Biol. **115:**97–107.

33. **Landschultz, W. H., P. F. Johnson, and S. L. McKnight.** 1988. The leucine zipper: a hypothetical structure common to a new class of DNA binding proteins. Science **240:**1759–1763.
34. **Lee, E. Y.-H. P., C.-Y. Chang, N. Hu, Y.-C. J. Wang, C.-C. Lai, K. Herrup,**

W.-H. Lee, and A. Bradley. 1992. Mice deficient for Rb are nonviable and show defects in neurogenesis and haematopoiesis. Nature (London) **359:** 288–294.
35. **Lee, W. H., R. Bookstein, F. Hong, L. J. Young, J. Y. Shew, and E. Y. Lee.** 1987. Human retinoblastoma susceptibility gene: cloning, identification, and sequence. Science **235:**1394–1399.
36. **Lemoine, N. R.** 1994. Molecular biology of breast cancer. Ann. Oncol. **5:**31–37.
37. **Levine, D. S., C. A. Sanchez, P. S. Rabinovitch, and B. J. Reid.** 1991. Formation of the tetraploid intermediate is associated with the development of cells with more than four centrioles in the elastase simian virus 40 tumor antigen transgenic mouse model of pancreatic cancer. Proc. Natl. Acad. Sci. USA **88:**6427–6431.
38. **Liao, H., G. Li, and T. J. Yen.** 1994. Mitotic regulation of microtubule cross-linking activity of CENP-E kinetochore protein. Science **265:**394–398.
39. **Ludlow, J. W., C. L. Glendening, D. M. Livingston, and J. A. DeCaprio.** 1993. Specific enzymatic dephosphorylation of the retinoblastoma protein. Mol. Cell. Biol. **13:**367–372.
40. **Mancini, M. A., and W.-H. Lee.** Unpublished data.
41. **Masumoto, H., Y. Masukata, N. Muro, N. Nozaki, and T. Okazaki.** 1989. A human centromere antigen (CENP-B) interacts with a short specific sequence in alphoid DNA, a human centromeric satellite. J. Cell Biol. **109:** 1963–1973.
42. **Minna, J. D.** 1993. The molecular biology of lung cancer pathogenesis. Chest **103:**449S–456S.
43. **Moroi, Y., C. Peebles, M. J. Fritzler, J. Styeigerwald, and E. M. Tan.** 1981. Autoantibody to centromere (kinetochore) in scleroderma sera. Proc. Natl. Acad. Sci. USA **77:**1627–1631.
44. **Nurse, P.** 1990. Universal control mechanism regulating onset of M-phase. Nature (London) **344:**503–508.
45. **Palmer, D. K., K. O'Day, H. L. Trong, and H. Charbonneau.** 1991. Purification of the centromere-specific protein CENP-A and demonstration that it is a distinctive histone. Proc. Natl. Acad. Sci. USA **88:**3734–3738.
46. **Pieke Dahl, H., et al.** 1993. Genetic heterogeneity of Usher syndrome type II. J. Med. Genet. **30:**843–848.
47. **Qian, Y.-W., Y.-C. J. Wang, R. E. Hollingsworth, Jr., D. Jones, N. Ling, and E. Y.-H. P. Lee.** 1993. A retinoblastoma-binding protein related to a negative regulator of ras in yeast. Nature (London) **364:**648–652.
48. **Rieder, C. L.** 1982. The formation, structure and composition of the mammalian kinetochore and kinetochore fiber. Int. Rev. Cytol. **79:**1–58.
49. **Saitoh, H., J. Tomkiel, C. A. Cooke, H. R. Ill, M. Maurer, N. F. Rothfield, and W. C. Earnshaw.** 1992. CENP-C, an autoantigen in scleroderma, is a component of the human inner kinetochore plate. Cell **70:**115–125.
50. **Sander, A., R. Schmelzle, and J. Murray.** 1994. Evidence for a microdeletion in 1q32-41 involving the gene responsible for Van Der Woude syndrome. Hum. Mol. Genet. **3:**575–578.
51. **Shan, B., C.-Y. Chang, D. Jones, and W.-H. Lee.** 1994. The transcription factor E2F-1 mediates the autoregulation of RB gene expression. Mol. Cell. Biol. **14:**299–309.
52. **Shan, B., X. Zhu, P.-L. Chen, T. Durfee, Y. Yang, D. Sharp, and W.-H. Lee.** 1992. Molecular cloning of cellular genes encoding retinoblastoma-associated proteins: identification of a gene with properties of the transcription factor E2F. Mol. Cell. Biol. **12:**5620–5631.
53. **Shenoy, S., J.-K. Choi, S. Bagrodia, T. D. Copeland, J. L. Maller, and D. Shalloway.** 1989. Purified maturation promoting factor phosphorylates pp60c-src at the sites phosphorylated during fibroblast mitosis. Cell **57:**763–774.
54. **Shew, J.-Y., N. Ling, X. Yang, O. Fodstad, and W.-H. Lee.** 1989. Antibodies detecting abnormalities of the retinoblastoma susceptibility gene product (pp110RB) in osteosarcomas and synovial sarcomas. Oncogene Res. **1:**205–214.
55. **Smith, D. B., and K. S. Johnson.** 1988. Single-step purification of polypeptides expressed in E. coli as fusions with glutathione S-transferase. Gene **67:**31–40.
56. **Steuer, E. R., L. Wordeman, T. A. Schroer, and M. P. Sheetz.** 1990. Localization of cytoplasmic dynein to mitotic spindles and kinetochores. Nature (London) **345:**266–268.
57. **Weinberg, R. A.** 1991. Tumor suppressor genes. Science **254:**1138–1146.
58. **Yan-Feng, T. L., G. Floyd-Smith, J. Drouin, and U. Francke.** 1985. Localization of pronatriodilatin gene to human chromosome 1 and mouse chromosome 4. Am. J. Hum. Genet. **37:**1117–1128.
59. **Yen, T. J., D. A. Compton, D. Wise, R. P. Zinkowski, B. R. Brinkley, W. C. Earnshaw, and D. W. Cleveland.** 1991. CENP-E, a novel human centromere-associated protein required for progression from metaphase to anaphase. EMBO J. **10:**1245–1254.
60. **Yen, T. J., G. Li, B. T. Schaar, I. Szilak, and D. W. Cleveland.** 1992. CENP-E is a putative kinetochore motor that accumulates just before mitosis. Nature (London) **359:**536–539.
61. **Zhu, X., K.-H. Chang, D. He, M.A. Mancini, W. R. Brinkley, and W.-H. Lee.** 1995. The C-terminus of mitosin is essential for its nuclear localization, centromere/kinetochore targeting and dimerization. J. Biol. Chem. **270:**1–6.
62. **Zieve, G. W., D. Turnbull, J. M. Mullins, and J. R. McIntosh.** 1980. Production of large numbers of mitotic mammalian cells by use of the reversible microtubule inhibitor nocodazole. Exp. Cell Res. **126:**397–405.

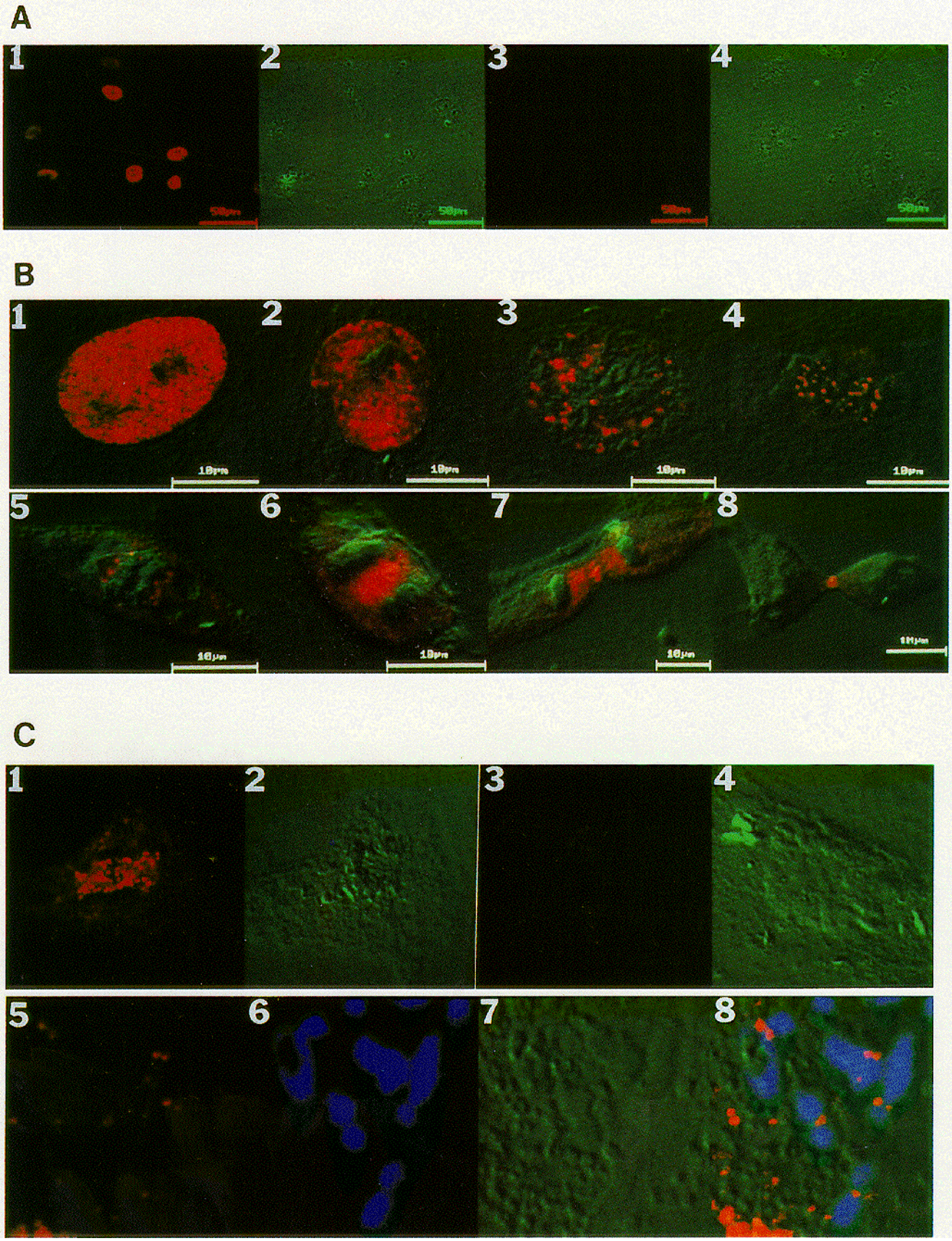
A
1
2
3
4
B
1
2
3
4
5
6
7
8
C
1
2
3
4
5
6
7
8

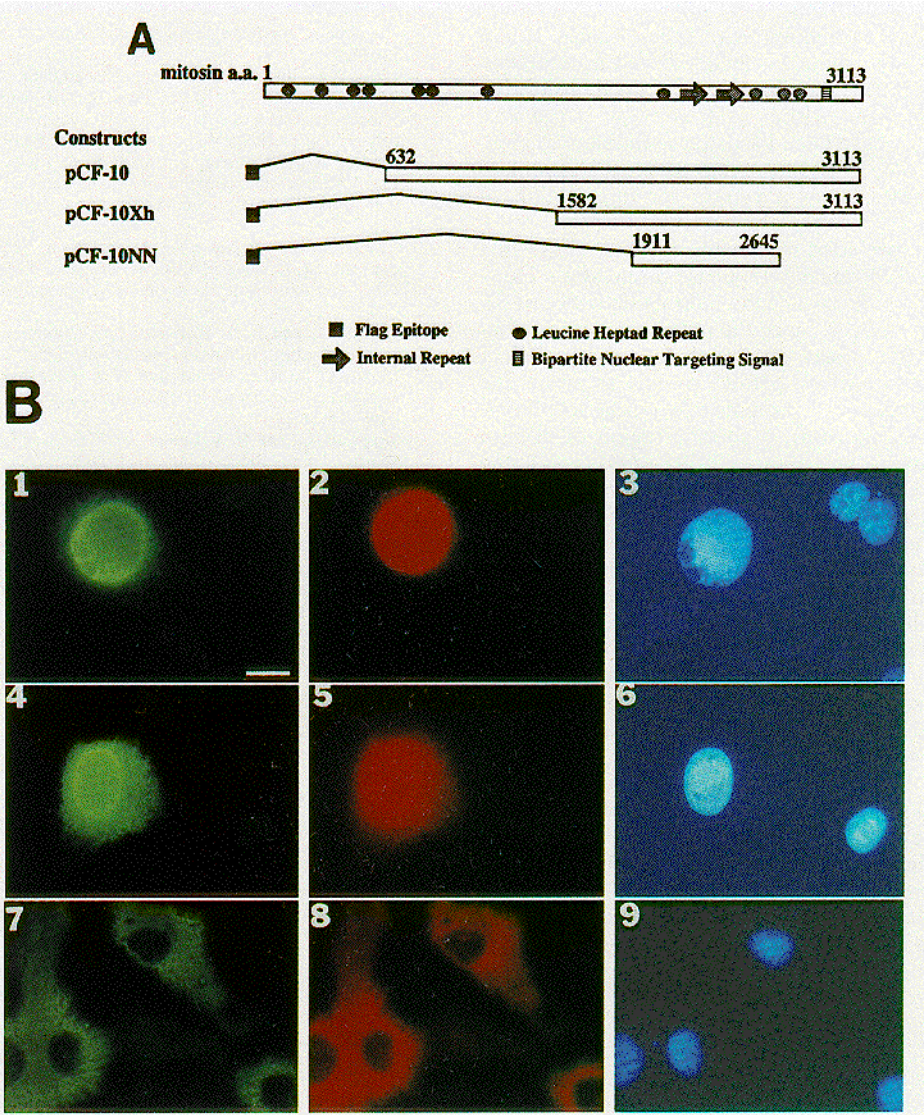
A
mitosin a.a. 1
3113
Constructs
pCF-10
632
3113
pCF-10Xh
1582
3113
pCF-10NN
1911
2645
Flag Epitope
Leucine Heptad Repeat
Internal Repeat
Bipartite Nuclear Targeting Signal
B
1
2
3
4
5
6
7
8
9